Inorg. Chem. **2006**, *45*, 10905–10908

Crystal Absorption Spectra in the Region of 4f–4f and 4f–5d Excitations in Tm^{2+}-Doped $CsCaCl_3$, $CsCaBr_3$, and $CsCaI_3$

Judith Grimm, Eva Beurer, and Hans U. GUdel*

Department of Chemistry and Biochemistry, University of Bern, Freiestrasse 3, 3012 Bern, Switzerland

Received November 11, 2005

Low-temperature absorption spectra of single crystals of Tm^{2+}-doped $CsCaCl_3$, $CsCaBr_3$, and $CsCaI_3$ in the spectral range from 8700 to 47000 cm^{-1} are presented. Weak sharp-line 4f–4f absorptions around 8800 cm^{-1} are essentially independent of the nature of the halide. More-intense broad absorptions cover the region between 12000 and 47000 cm^{-1}. They are assigned to 4f–5d excitations and interpreted in terms of a simple qualitative picture taking into account the most important interactions. As a result of two counterbalancing effects, the onsets of the 4f–5d spectra are almost coincident in the three materials: The blue-shift of about 3000 cm^{-1} between chloride and iodide resulting from the decreasing crystal field splitting of 5d is roughly balanced by the red-shift resulting from the reduced energy gap between the average energy of the $4f^{13}$ and the $4f^{12}5d^1$ electron configurations. The absorption helps the understanding of the most unusual light emission properties of these materials.

1. Introduction

Studies on the optical spectroscopic properties of divalent lanthanides have mainly concentrated on Eu^{2+}, Yb^{2+}, and Sm^{2+}, as these are readily stabilized in the divalent oxidation state.[1] By far, the most comprehensive literature is found for Eu^{2+}. The luminescence of Eu^{2+} has been intensively studied, as this ion plays an important role in phosphor materials for fluorescent lighting.[2] In Sm^{2+}-doped crystals, room-temperature persistent spectral hole burning was demonstrated for the first time.[3] The 5d-to-4f transitions of Yb^{2+} are of interest for possible laser applications.[4] In contrast, spectroscopic studies of Tm^{2+} are rather scarce. This mainly reflects the greater difficulties that are encountered when trying to stabilize this ion in its divalent state in an oxide or fluoride environment. In the heavier halides, the situation is thermodynamically more favorable, and we have recently presented the light emission properties of Tm^{2+} doped into $CsCaBr_3$.[5] An unusually rich variety of light emissions was discovered in this system. Five different types of transitions were found to coexist and compete as a function of temperature. We are extending these studies to include other host lattices and find that the Tm^{2+} light emission properties exhibit a great deal of variation depending on the host.[6] Besides the light emission, the absorption properties are of great interest because they are essentially unexplored.

In the present contribution, we offer a comparative study of the absorption spectra from the near-infrared (NIR) to the ultraviolet (UV) of Tm^{2+} in the perovskite host lattices $CsCaCl_3$, $CsCaBr_3$, and $CsCaI_3$. Both 4f−4f and 4f−5d excitations are observed from the NIR to the UV, and the chemical variation mainly affects the latter through the direct exposure of the 5*d* electron to the octahedral halide coordination. The experimental results are discussed semiquantitatively by identifying the dominant interactions but without an attempt to model the data quantitatively. This is the first systematic study of the 4f−4f and 4f−5d excitations of Tm^{2+} in a series of related host lattices.

2. Experimental Section

Single crystals of $CsCaCl_3$, $CsCaBr_3$, and $CsCaI_3$ doped with Tm^{2+} were grown by the Bridgman technique. For the synthesis, stoichiometric amounts of CsX (X = Cl, Br, I) and CaX_2 were

* To whom correspondence should be addressed. Email: hans-ulrich.guedel@iac.unibe.ch. Phone: ++41 31 631 42 49. Fax: ++41 31 631 43 99.

(1) Rubio, J. *J. Phys. Chem. Solids* **1991**, *52*, 101.
(2) Blasse, G.; Grabmeier, B. C. *Luminescent Materials*; Springer-Verlag: Berlin, 1994.
(3) Holliday, K.; Wei, C.; Croci, M.; Wild, U. P. *J. Lumin.* **1992**, *53*, 227.
(4) Kück, S. *Appl. Phys. B* **2001**, *72*, 515.
(5) Grimm, J.; Güdel, H. U. *Chem. Phys. Lett.* **2005**, *404*, 40.
(6) Grimm, J.; Suyver, J. F.; Beurer, E.; Carver, G.; Güdel, H. U. *J. Phys. Chem. B* **2006**, *110*, 2093.

10.1021/ic051951m CCC: $33.50
Published on Web 12/07/2006

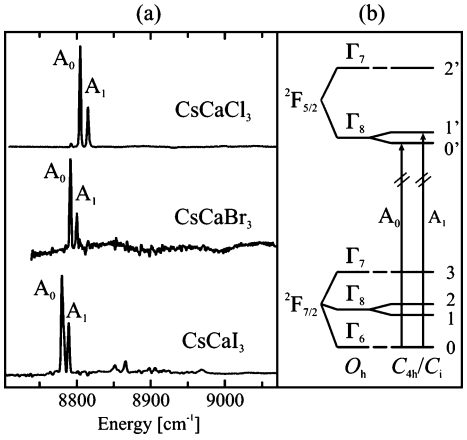

Figure 1. (a) 10 K absorption spectrum of $CsCaCl_3$:1.04% Tm^{2+}, $CsCaBr_3$: 0.48% Tm^{2+}, and $CsCaI_3$:0.76% Tm^{2+} in the region of the 4f−4f excitations. (b) Schematic energy level diagram of the $^2F_{7/2} \rightarrow {}^2F_{5/2}$ transition. The arrows indicate the transitions that are observed in (a).

mixed. Tm^{2+} was prepared in situ by synproportionation of TmX_3 and Tm metal. The use of Ta ampules is indispensable for the success of the synthesis. Crystals grown from silica ampules contain trace amounts of Tm^{3+} because under such crystal growth conditions Tm^{2+} is easily oxidized by silica. The absolute concentration of Tm is 1.04%, 0.48%, and 0.76% in $CsCaCl_3$, $CsCaBr_3$, and $CsCaI_3$, respectively, and was determined by ICP-OES. Due to their hygroscopic nature, the handling of the starting materials, as well as the crystals, occurred under inert atmosphere at all times. For absorption measurements, the samples were polished in a drybox and enclosed in an airtight copper cell. Absorption spectra were recorded on a Cary 6000i spectrometer (Varian). Sample cooling was achieved with a closed-cycle cryostat (Air Products).

3. Results

$CsCaCl_3$:1.04% Tm^{2+}, $CsCaBr_3$:0.48% Tm^{2+}, and $CsCaI_3$: 0.76% Tm^{2+} are dark green crystals. Figure 1a shows sections of the 10 K crystal absorption spectra of finely polished crystals in the region of the 4f−4f excitations between 8700 and 9100 cm^{-1} in the NIR. Except for a very slight red-shift within the series from chloride to iodide, there is little variation in these sharp-line spectra.

Figure 2 shows the absorption spectra extending from 13 000 cm^{-1} in the NIR to 47 000 cm^{-1} in the UV. This is the region of 4f−5d excitations, and it is most unusual that absorption spectra of allowed transitions can be measured over such a broad spectral range. Usually, big variations in absorption intensities prevent this. The spectra in Figure 2 show a rich structure with bands of similar widths and intensities. A first-sight comparison of the three spectra reveals both similarities and differences. The first, and perhaps surprising, observation is that the onset of the 4f−5d bands in the NIR does not differ by more than about 1000 cm^{-1} in the three systems. The low-energy part of the spectra is shown on an expanded scale in Figure 3 for better comparison. It shows that not only the onset but also the appearance of the spectra up to about 23 000 cm^{-1} are similar for the three compounds. Above 23 000 cm^{-1}, the similarity becomes less pronounced, and in particular, the shape of the $CsCaI_3$:Tm^{2+} spectrum deviates from the other two.

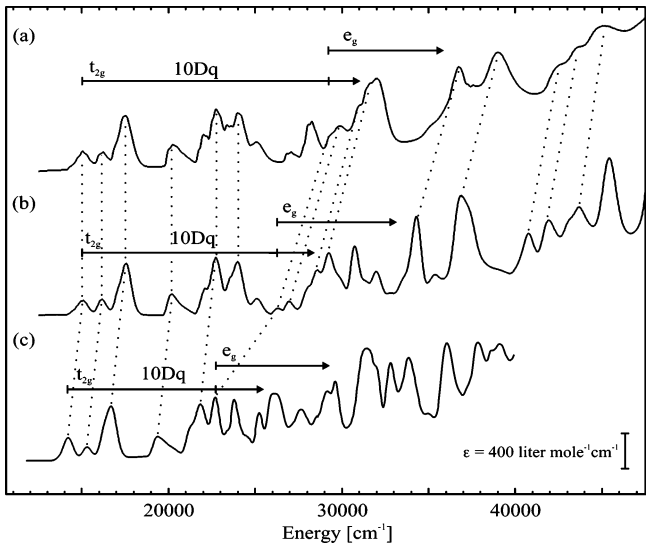

Figure 2. Single-crystal absorption spectra in the region of the 4f−5d transitions of (a) $CsCaCl_3$:1.04% Tm^{2+}, (b) $CsCaBr_3$:0.48% Tm^{2+}, and (c) $CsCaI_3$:0.76% Tm^{2+} recorded at 10 K. The spectra are corrected for the Tm^{2+} concentration to have the same ϵ (molar extinction coefficient) scales, see bottom right. Corresponding bands are connected by dotted lines, and the onset of absorption bands corresponding to the ($^3H_6$,t_{2g}) and ($^3H_6$,e_g) multiplets are marked with t_{2g} and e_g arrows.

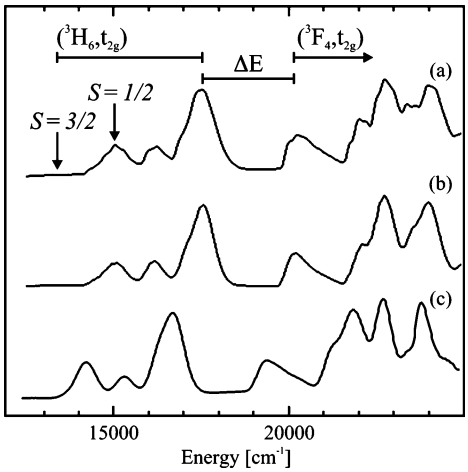

Figure 3. 10 K absorption spectrum of (a) $CsCaCl_3$:1.04% Tm^{2+}, (b) $CsCaBr_3$:0.48% Tm^{2+}, and (c) $CsCaI_3$:0.76% Tm^{2+} in the region of the onset of the 4f−5d absorption transitions. The assignment of the bands is given on top of the $CsCaCl_3$:Tm^{2+} spectrum. The first S = 1/2 and S = 3/2 transitions within ($^3H_6$,t_{2g}) are marked with arrows. ΔE defines the gap between the highest absorption within the ($^3H_6$,t_{2g}) multiplet and the lowest component of ($^3F_4$,t_{2g}).

4. Discussion

4.1. Host Materials. $CsCaCl_3$ and $CsCaBr_3$ are cubic perovskites at room temperature (space group *Pm*3*m*) with Ca^{2+} on a site with O_h symmetry. Both materials undergo phase transitions at lower temperatures.[7,8] At 10 K, $CsCaCl_3$ and $CsCaBr_3$ crystallize as tetragonal (space group *P*4/*mbm*) and orthorhombic (space group *Pnma*) phases, respectively. $CsCaI_3$ is stable in the orthorhombic *Pnma* space group at all temperatures between 10 and 300 K. At 10 K, the Ca^{2+} site symmetry is C_{4h} in $CsCaCl_3$ and C_i in $CsCaBr_3$ and $CsCaI_3$. In all cases, the distortions of the octahedral CaX_6

(7) Seifert, H.-J.; Langenbach, U. *Z. Anorg. Allg. Chem.* **1969**, *368*, 36.
(8) Seifert, H.-J.; Haberhauer, D. *Z. Anorg. Allg. Chem.* **1982**, *491*, 301.

coordination are very small, and in the crystal spectra, their effect only shows up in the highly resolved 4f−4f absorptions of the Tm^{2+}-doped materials, in which Tm^{2+} substitutes for Ca^{2+}. O_h notation will therefore be used in the discussion of the 4f−5d excitations.

4.2. 4f−4f Excitations. Tm^{2+} has a $4f^{13}$ ground-state electron configuration, resulting in a $^2F_{7/2}$ ground term and a $^2F_{5/2}$ excited term, see Figure 1b. This is in exact analogy to the situation in Yb^{3+}, whose spectroscopic properties have been well explored in a variety of chemical environments. Since the spin−orbit coupling is smaller in Tm^{2+}, the $^2F_{7/2} \leftrightarrow {}^2F_{5/2}$ transitions, both in absorption and emission and independent of the chemical environment, are shifted from about 10 000 cm^{-1} in Yb^{3+} to about 8800 cm^{-1} in Tm^{2+}.[9,10] This is seen in Figure 1a.

The absorption spectra in Figure 1a are dominated by the sharp lines A_0 and A_1, which show a red-shift of 16 cm^{-1} between the chloride and iodide. Both A_0 and A_1 are assigned to electronic origins, as shown in Figure 1b, from their coincidence with corresponding cold emission lines. The red-shift along the halide series is a result of the decreasing spin−orbit coupling strength, caused by the increasing covalency. Since Tm^{2+} occupies a centrosymmetric site in all the lattices, the transitions A_0 and A_1 arise by a magnetic dipole (MD) mechanism. Γ_6 to Γ_8 (O_h notation) is MD allowed, while Γ_6 to Γ_7 is forbidden. This explains the dominance of A_0 and A_1 in the spectra. It is not possible to unambiguously assign any of the other features to the Γ_6-to-Γ_7 origin. The small splitting of 8 or 9 cm^{-1} between A_0 and A_1 results from the splitting of Γ_8 into the two Kramers doublets *0′* and *1′* and thus reflects the small distortion of the TmX_6 octahedron below the phase transitions.

4.3. 4f−5d Excitations. Yb^{3+}-doped oxides, fluorides, chlorides, and bromides are completely transparent between about 10 000 and 30 000 cm^{-1}. This property makes Yb^{3+} an important sensitizer ion for photon upconversion in Er^{3+}- and Tm^{3+}-doped systems.[11,12] The first allowed optical excitations of Yb^{3+} in the UV are of the ligand-to-metal charge transfer (LMCT) type, and only at higher energies 4f−5d absorptions occur.[13] In contrast, Tm^{2+} shows intense absorptions with ϵ values of the order of 1000 $L(mol \cdot cm)^{-1}$ throughout the visible (VIS) and UV region, see Figure 2.[14,15] These are due to 4f−5d excitations, which are shifted to lower energies by about 50 000 cm^{-1} compared to Yb^{3+}. LMCT transitions, on the other hand, are expected to shift to higher energies in Tm^{2+}, and we do not consider them in our discussion of Figure 2.

A red-shift of 30 000−50 000 cm^{-1} in the 4f−5d excitations of divalent lanthanides compared to their isoelectronic trivalent counterparts is observed throughout the lanthanide series.[16,17] This is a result of the reduced Coulomb attraction of the 5d electron by the nucleus in the divalent ions, which leads to a reduced energy separation of 5d and 4f. All the absorption bands shown in Figure 2 between 13 000 and 47 000 cm^{-1} can thus be assigned to 4f−5d excitations.

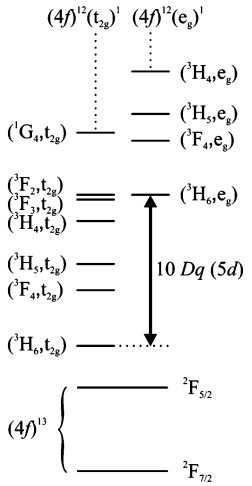

Figure 4. Schematic energy splittings of the $4f^{13}$ and $4f^{12}5d^1$ electron configurations in Tm^{2+}. For the $4f^{12}5d^1$, only the interactions $H_{CF}(d)$ and $H_{Coul+SO}(f)$, as defined in the text, are considered. The levels derived from $4f^{12}t_{2g}^1$ and $4f^{12}e_g^1$ are displayed separately for better distinction.

The $4f^{12}5d^1$ electron configuration has a total degeneracy of 910. This is split by a variety of interactions. For Tm^{2+}, the four most important interactions are[18,19]

$$H = H_{CF}(d) + H_{Coul+SO}(f) + H_{Coul}(fd) + H_{SO}(d)$$

(i) $H_{CF}(d)$, crystal field interaction of the 5d electron; (ii) $H_{Coul+SO}(f)$, combined Coulomb repulsion and spin−orbit coupling within the $4f^{12}$ configuration; (iii) $H_{Coul}(fd)$, Coulomb repulsion of the 4f and 5d electrons; and (iv) $H_{SO}(d)$, spin−orbit interaction of the 5d electron.

$H_{CF}(d)$ splits the 5d orbital into t_{2g} and e_g sets of octahedral orbitals separated by 10 *Dq*. The effect of $H_{Coul+SO}(f)$ is to split the $4f^{12}$ configuration into $^{2S+1}L_J$ terms very similar to the situation in Tm^{3+}, represented in the well-known Dieke diagram.[20] This leads to a situation depicted schematically in Figure 4. The multiplets in Figure 4 will then be further split by $H_{Coul}(fd)$ and $H_{SO}(d)$.

With this relatively simple picture in mind, we are able to interpret the low-energy part of the spectra in Figure 2. The spectra of $CsCaCl_3$:Tm^{2+} and $CsCaBr_3$:Tm^{2+} are very similar up to 26 200 cm^{-1}, where a new band appears in the bromide spectrum. And in $CsCaI_3$:Tm^{2+}, the first new band appears at 22 800 cm^{-1}. All the bands at lower energies can be assigned to excited states deriving from the $4f^{12}t_{2g}^1$ electron configuration, and we take the appearance of the first new band as the onset of the $4f^{12}e_g^1$ ladder, see right-hand side of Figure 4. This assignment is confirmed by the

(9) Kiss, Z. J. *Phys. Rev.* **1962**, *127*, 718.
(10) Wenger, O. S.; Wickleder, C.; Krämer, K. W.; Güdel, H. U. *J. Lumin.* **2001**, *94*−*95*, 101.
(11) Suyver, J. F.; Aebischer, A.; Biner, D.; Gerner, P.; Grimm, J.; Heer, S.; Krämer, K. W.; Reinhard, C.; Güdel, H. U. *Opt. Mater.* **2005**, *27*, 1111.
(12) Auzel, F. *Chem. Rev.* **2004**, *104*, 139.
(13) van Pieterson, L.; Heeroma, M.; de Heer, E.; Meijerink, A. *J. Lumin.* **2000**, *91*, 177.
(14) Loh, E. *Phys. Rev.* **1968**, *175*, 533.
(15) Alig, R. C.; Duncan, R. C.; Mokross, B. J. *J. Chem. Phys.* **1973**, *59*, 5837.
(16) Dorenbos, P. *J. Phys. Cond. Matter* **2003**, *15*, 575.
(17) Dorenbos, P. *J. Lumin.* **2000**, *91*, 155.
(18) Dorenbos, P. *J. Phys. Cond. Matter* **2003**, *15*, 6249.
(19) Duan, C. K.; Reid, M. F. *J. Solid State Chem.* **2003**, *171*, 299.
(20) Dieke, G. H. *Spectra and Energy Levels of Rare Earth Ions in Crystals*; John Wiley and Sons: New York, 1968.

Table 1. Compiled Key Data of Tm^{2+}-Doped $CsCaCl_3$, $CsCaBr_3$, and $CsCaI_3$[a]

	$CsCaCl_3$	$CsCaBr_3$	$CsCaI_3$
10 *Dq* [cm^{-1}]	14 200	11 200	8500
($^3H_6$,t_{2g})S = 3/2 [cm^{-1}]	13 092	13 256	12 348
($^3H_6$,t_{2g})S = 1/2 [cm^{-1}]	15 036	15 077	14 155
($^3F_4$,t_{2g}) [cm^{-1}]	20 245	20 196	19 337
($^3H_6$,e_g) [cm^{-1}]	29 266	26 281	22 695
ΔE [cm^{-1}]	2760	2620	2700

[a] 10 *Dq* is the crystal-field splitting of the 5d part of the $4f^{12}5d^1$ electron configuration. The first spin-forbidden and spin-allowed transitions within the ($^3H_6$,t_{2g}) multiplet are given, as well as the first transition of ($^3F_4$,t_{2g}) and the first ($^3H_6$,e_g) transition. ΔE is the energy separation between the highest component of the ($^3H_6$,t_{2g}) and the lowest component of the ($^3F_4$,t_{2g}) multiplets.

correspondence between equivalent bands connected by dotted lines for the chloride and bromide in Figure 2. For the iodide, the analogy to the chloride and bromide spectra ends above 23 000 cm^{-1}. On the basis of this assignment, we are able determine the crystal-field parameter 10 *Dq* for the title compounds, see Table 1.

The decrease of 10 *Dq* from chloride to iodide of 40% would predict a corresponding blue-shift of the 4f−5d bands of about 3000 cm^{-1}. However, we observe slight red-shifts of less than 1000 cm^{-1} in the low-energy part of the absorption spectrum (see Figure 3). The $CsCaCl_3$:Tm^{2+} and $CsCaBr_3$:Tm^{2+} absorption spectra are essentially superimposable between 13 000 and 25 000 cm^{-1}. It clearly demonstrates that the decrease of 10 *Dq* is counterbalanced by a decrease of the energy separation between the centers of gravity of the $4f^{13}$ and the $4f^{12}5d^1$ electron configurations. This shift of the average 4f−5d transition energy can result from several interactions such as the polarizability of the ligands, covalency, and others.[21] Between the chloride and the bromide, the two effects happen to cancel exactly at the onset of the 4f−5d absorption spectrum.

In the low-energy part of the spectra in Figure 3, we can push the interpretation of the observed bands a bit further. The effect of $H_{Coul+SO}$(f) can be identified. The lowest terms arising from $4f^{12}t_{2g}^1$ under the action of $H_{Coul+SO}$(f) are ($^3H_6$,t_{2g}) and ($^3F_4$,t_{2g}), see the left column in Figure 4. In Tm^{3+}, $^3F_4$ lies about 5550 cm^{-1} above $^3H_6$, and thus, we expect the onset of ($^3F_4$,t_{2g}) at about 19 700 cm^{-1} in the chloride and bromide and at about 18 700 cm^{-1} in the iodide in our absorption spectra. This is nicely borne out, as shown in Figure 3, where the assignment is given for the chloride. ($^3H_6$,t_{2g}) consists of numerous absorption bands and covers an energy range of about 4000 cm^{-1}. An energy gap, ΔE, of about 2700 cm^{-1} separates the lowest component of ($^3F_4$,t_{2g}) from the highest component of ($^3H_6$,t_{2g}) in all three samples, see Figure 3 and Table 1. This gap is large enough for the lowest component of ($^3F_4$,t_{2g}) to become metastable and emissive, particularly in the bromide and iodide.[6] At higher energies, there is no energy gap of this order of magnitude. Increasing overlap of bands toward higher energies makes an unambiguous assignment of ($^{2S+1}L_J$,t_{2g}) and ($^{2S+1}L_J$,e_g) terms impossible.

The energy splittings within the ($^3H_6$,t_{2g}) multiplet arise from the interactions H_{Coul}(fd) and H_{SO}(d). The isotropic part of H_{Coul}(fd) causes a splitting into a set of states with spin S = 1/2 and another with S = 3/2. From the absorption and emission spectra, we conclude that S is still a reasonably good quantum number within ($^3H_6$,t_{2g}): The lowest-energy 4f−5d absorption band is very weak in all the three spectra, and we assign it to a spin-forbidden $^2F_{7/2} \rightarrow$ ($^3H_6$,t_{2g})S = 3/2 transition. This lowest excited 4f−5d state is emissive in all three compounds.[6] As shown in Figure 3 and listed in Table 1, the first intense absorption band lies about 2000 cm^{-1} higher in energy and is assigned to the lowest energy spin-allowed $^2F_{7/2} \rightarrow$ ($^3H_6$,t_{2g})S = 1/2 excitation. This state is also metastable up to room temperature in the bromide and iodide and shows a very weak short-lived emission.[5,6] From the experiment-based distinctions between spin-forbidden and spin-allowed transitions within the ($^3H_6$,t_{2g}) multiplet, we conclude that the effect of H_{SO}(d) is weaker than that of H_{Coul}(fd). In the higher-energy multiplet ($^3F_4$,t_{2g}), such a distinction is no longer possible as the lowest-energy absorption band is intense. [18]

5. Conclusions

This study shows that, in contrast to oxide and fluoride lattices, Tm^{2+} is easily incorporated into crystal lattices of the heavier halides. The synthesis of sizable crystals of Tm^{2+}-doped $CsCaCl_3$, $CsCaBr_3$, and $CsCaI_3$ perovskites allows a systematic study of the 4f−4f and 4f−5d excited-state properties by absorption spectroscopy. This is an essentially unexplored area. By their location in the VIS and near-UV part of the spectrum, the 4f−5d excitations are experimentally easily accessible. This is in contrast to trivalent lanthanides, in which 4f−5d absorptions are usually in the vacuum UV and thus more difficult to explore. Tm^{2+} offers another significant advantage for the study of 4f−5d excitations. There is only one 4f−4f excited state within the $4f^{13}$ electron configuration, $^2F_{5/2}$, and it lies around 8800 cm^{-1}, so that the whole spectral range between 12000 and 47000 cm^{-1} covered in the present study consists of pure 4f−5d excitations, without any interference from higher 4f−4f excited states. In ref 6, we show that the light-emission properties of the title materials are unusual and interesting, possibly also with respect to future applications. A particularly interesting feature is the unprecedented observation of light-emission from higher-excited 4f−5d states and the resulting occurrence of upconversion processes.[22] The present study helps to clarify the excited-state situation. It also shows that a reasonable level of understanding can be achieved using a very simple picture, without trying to model all the excited-state splittings quantitatively.

IC051951M

(21) Andriessen, J.; Dorenbos, P.; van Eijk, C. W. E. *Phys. Rev. B* **2005**, *72*, 045129

(22) Beurer, E.; Grimm, J.; Gerner, P.; Güdel, H. U. *J. Am. Chem. Soc.* **2006**, *128*, 3110.